Journal of
Nanoscience and Nanotechnology
Vol. 9, 7012–7015, 2009

Statistical Analysis of Metal-Molecule Contacts in Alkyl Molecular Junctions: Sulfur versus Selenium End-Group

Hana Yoo[1], Jungseok Choi[2], Gunuk Wang[1], Tae-Wook Kim[1], Jaegeun Noh[2], and Takhee Lee[1,*]

[1] Department of Materials Science and Engineering, Gwangju Institute Science and Technology, Gwangju 500-712, Korea
[2] Department of Chemistry, Hanyang University, 17 Haengdang-dong, Seongdong-gu, Seoul 133-791, Korea

We fabricated a large number of microscale via-hole structure molecular devices (2240 devices) using octane-Se [$CH_3(CH_2)_7Se$] self assembled monolayers (SAMs) and compared their charge transport properties with those of octane-S [$CH_3(CH_2)_7S$] SAMs molecular devices in terms of current density, resistance, and tunneling decay coefficient. The device yield of the "working" octane-Se molecular devices was found to be ~1.7% (38/2240), which was similar to the yield of ~1.1% (50/4480) for octane-S devices. Our statistical analysis revealed that for octane-Se devices the tunneling current was slightly smaller and the low-bias resistance and decay coefficient were slightly larger than those for octane-S devices. The standard deviations of these transport parameters of octane-Se devices were found to be broader than those for octane-S devices due to irregularity of the binding sites of octane-Se on Au electrode surface.

Keywords: A Molecular Electronics, Device Yield, Alkanethiols.

1. INTRODUCTION

Molecular electronics utilizing functional organic molecules as the ultimate nanoscale electronic components have demonstrated their potential in device applications for ultrahigh density future electronics.[1–7] The role of the metal-molecule contact in the electronic transport through organic molecules sandwiched between metallic electrodes is currently an important issue in the field of molecular electronics.[8–14] Furthermore, for the quantitative understanding of metal-molecule contact properties, the statistical analysis of electronic transport properties is important since it can give more accurate characteristics of a molecular system.[15–17]

Here, we report the influence of the metal-molecule contact on the electronic transport properties in alkyl metal-molecule-metal (M-M-M) junctions. Specifically, we investigated two different metal-molecule contacts in terms of different molecular end-groups; octane-Se (having Se end-group) and octane-S (having S end-group) in alkyl M-M-M devices. From the statistical analysis of a large number of molecular devices, we compared the transport parameters such as tunneling current densities, resistances, and decay coefficients for octane-Se versus octane-S molecular systems.

2. EXPERIMENTAL DETAILS

The octane-Se [$CH_3(CH_2)_7Se$] and octane-S [$CH_3(CH_2)_7S$] M-M-M junction devices were fabricated on a *p*-type (100) Si substrate which is covered with thermally grown 3000 Å thick SiO_2. As shown in Figure 1, the conventional optical lithography method was used to pattern bottom electrodes that was made with Au (1000 Å)/Ti (50 Å) by an electron beam evaporator. Next, the patterned bottom electrodes were deposited by SiO_2 layer (700 Å thick) using plasma enhanced chemical vapour deposition (PECVD). And then, reactive ion etching (RIE) was performed to make micro-via holes of 2 μm diameter through SiO_2 layer to expose Au surfaces. Molecules were used to form the active molecular component. The chips were left in the 1 mM and 5 mM molecular solution

*Author to whom correspondence should be addressed.

 1533-4880/2009/9/7012/004 doi:10.1166/jnn.2009.1620

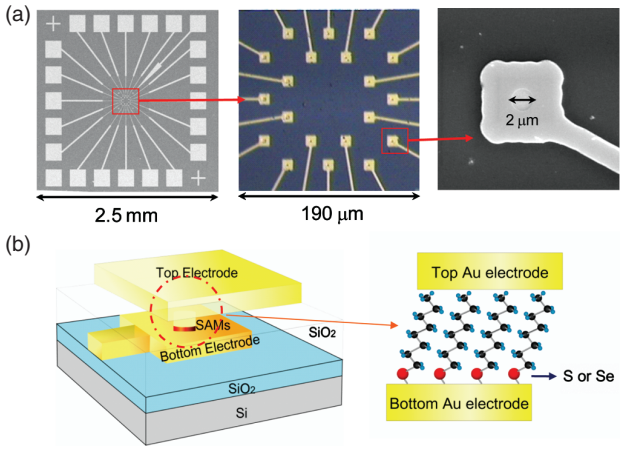

Fig. 1. (a) Optical and SEM images of fabricated molecular devices and (b) schematics of a micro-via hole molecular device. The junction is ~2 μ in diameter.

for 24 h for the octane-Se and octane-S self-assembled monolayers (SAMs), respectively, to assemble on the Au surfaces exposed by RIE in a nitrogen-filled glove box with an oxygen level of less than ~10 ppm. Octane-Se and octane-S SAMs were formed on exposed Au surfaces, and the top Au electrode was produced by thermal evaporator to form M-M-M junctions. This evaporation was done with a shadow mask on the chips with a water cooled cold stage in order to avoid thermal damage to the active molecular component under the pressure of $\sim 10^{-6}$ torr. For the same reason, the deposition rate of a top Au electrode was kept very low, typically at ~0.1 Å/s and the total Au thickness was ~500 Å. Figure 1 shows the optical images and schematics of microscale M-M-M junction devices having different end-groups of S and Se on the bottom Au surface. Room temperature current–voltage (I–V) characteristics of the fabricated molecular devices were measured using semiconductor characterization systems (Keithley 4200-SCS and HP4155A).

3. RESULTS AND DISCUSSION

We fabricated and characterized a significantly large number of molecular devices (2240 octane-Se devices and 4480 octane-S devices) to statistically analyze the molecular electronic properties. Majority of the fabricated devices showed short-circuit ohmic I–V characteristics with an electrical short when a current is larger than a few milliamperes,[18] and some devices showed noisy and open-circuit I–V behaviours. But among these fabricated devices, a sufficient number of devices were considered as "working" molecular electronic devices (see Table I). The working devices displaying molecular properties were determined based on the statistical distribution of the current densities of the fabricated devices.[15] Basically, the working molecular electronic devices were extracted from the devices showing a majority of current densities in

Table I. Summary of results for the fabricated devices.

Molecule	#of device	Fab. failure	Short	Open	Non-working	Working
Octane-S	4480	81	3969	346	34	50
	(100%)	(1.8%)	(88.6%)	(7.7%)	(0.8%)	(1.1%)
Octene-Se	2240	31	1733	433	5	38
	(100%)	(1.4%)	(77.4%)	(19.3%)	(0.2%)	(1.7%)

Note: Working devices were defined by statistical analysis with Gaussian fitting on histograms of the logarithmic scale current densities (see text).

the statistical distribution by using a Gaussian function (Fig. 2(a)). Here, we treated the working devices as those located within 1σ around mean value (m), where σ is standard deviation from the Gaussian fitting. More detail criterion for determining working devices has been reported elsewhere.[15] From Figure 2(a), the values of {m and σ} for the logarithmic current densities (in the unit of A/cm^2) at 1 V for octane-S and octane-Se were found to be {4.87 and 0.23} and {4.66 and 0.55}, respectively, which correspond the mean current densities of 7.2×10^4 for octane-S and 4.8×10^4 A/cm^2 for octane-Se. Table I summarizes the status of the fabricated devices and device yield. As summarized in this table, the number of octane-S and octane-Se working devices were determined as 50 and 38, respectively, among the total 6720 (4480 + 2240) fabricated devices. Thus, the device yields were found as ~1.1% (50/4480) for octane-S and ~1.7% (38/2240) for octane-Se devices. Since the device yield of octane-Se devices is not much different from that of octane-S devices, this result suggests that device yield is not much affected by the metal-molecule contact, i.e., the different molecular end-groups in our study, instead the molecular structure and device structure are more responsible for the overall device yield. Note that the use of a statistical

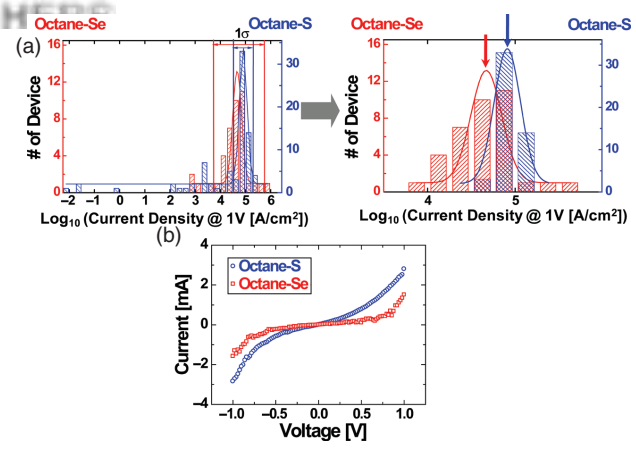

Fig. 2. (a) (left) Histograms of logarithmic current densities at 1 V for octane-S and octane-Se molecular devices with the Gaussian fitting curves. The solid lines (1 μg range) indicate the range of the working molecular devices. (right) Histograms for the working molecular devices only with the representative devices marked with arrows. (b) I–V characteristics of representative octane-S and octane-Se molecular devices.

approach in this study is very significant, as the analysis of a large number of devices increases the ability to develop more accurate and meaningful characteristics of molecular systems.

The right figure in Figure 2(a) presents the statistical histograms of current densities in logarithmic scale for different contacts of octane molecules (S and Se) at 1.0 V for only the working devices with the mean positions as the "representative devices" indicated with arrows form the fitting results by Gaussian functions. Figure 2(b) shows the I–V characteristics for the two selected representative. Even though some theoretical groups reported that Se is a better electronic coupling group than S,[19] our result showed the conductance for octane-Se devices was slightly lower than that for octane-S devices. This discrepancy could be because the binding sites of Se end-group on the bottom Au surface are more sensitive to molecular concentration, temperature, and deposition time for SAM formation on Au than S end-group.[27–29] The S end-group (known as thiol) has been reported to form a very stable monolayer on Au surface.[28, 30] Therefore, the Se end-group causes more irregularity in the octane-Se SAMs on Au.[27–29] This can be supported by Figures 2 and 3 in which the octane-Se devices exhibited a larger distribution of current and decay coefficient (β) values than those for octane-S devices. The irregularity of octane-Se SAM formation may cause this large statistical distribution of transport behaviors for the octane-Se devices.

We investigated the electron transport through different contact molecules with the Simmons tunneling model, a widely used model for describing a rectangular tunneling barrier. Many research groups have demonstrated that the charge transport through alkyl SAMs is tunneling and can be explained by the Simmons tunneling model[21–24] as

$$J = \left(\frac{e}{4\pi^2\hbar\, d^2}\right)\left\{\left(\Phi_B - \frac{eV}{2}\right)\exp\left[-\frac{2(2m)^{1/2}}{\hbar}\cdot\alpha\left(\Phi_B - \frac{eV}{2}\right)^{1/2} d\right] - \left(\Phi_B + \frac{eV}{2}\right)\cdot\exp\left[-\frac{2(2m)^{1/2}}{\hbar}\alpha\left(\Phi_B + \frac{eV}{2}\right)^{1/2} d\right]\right\} \quad (1)$$

where m is the electron mass, d is the barrier width, Φ_B is the barrier height, V is the applied bias, and α is a unit less adjustable parameter that may be used to differentiate between potential barrier shapes, or to describe effective electron mass. The molecular lengths used in this work are 13.3 Å for octane-S and 13.6 Å for octane-Se which were determined by adding an Au-sulfur and selenium bonding length to the length of molecule.[25] The electrical parameters of Φ_B, α, β, and current density (J) at 1 V for octane-S and octane-Se devices are summarized in Table II. The optimum fitting parameters were statistically determined as $\Phi_B = 1.08 \pm 0.26$ eV and $\alpha = 0.77 \pm 0.08$, $\Phi_B = 1.15 \pm 0.22$ eV and $\alpha = 0.76 \pm 0.12$ from all the working octane-S and octane-Se devices, respectively. Figure 3(b) shows the histograms of β values which were calculated from the Simmons fitting results, Φ_B and α values, for all the working octane-S and octane-Se devices. The current densities of alkyl molecules are known to exhibit an exponential length dependent transport, characterized by a tunneling decay coefficient β.[1, 11, 21, 26, 27] This β value can be expressed in the low bias range from the Simmons equation (Eq. (1)) as

$$\beta = \frac{2(2m)^{\frac{1}{2}}}{\hbar}\alpha(\Phi_B)^{\frac{1}{2}} \quad (2)$$

The β values were calculated for all of the individual working devices and were summarized as histograms in Figure 3(b). A slight increase in β values with octane-Se can be seen in this figure, which means that the electronic tunneling is slightly inefficient for the octane-Se junction case than the octane-S junction case.

We also calculated the resistance of each working device octane-S and 1.87 ± 1.45 kΩ for octane-Se devices. Resistance of octane-Se devices was slightly larger than that of octane-S devices. The standard deviation of resistances for

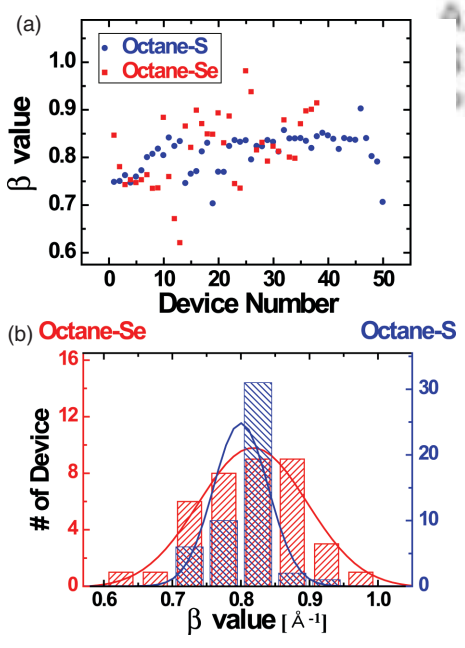

Fig. 3. (a) Distributions of β values and (b) histograms of β values for octane-S and octane-Se working molecular devices.

Table II. Summary of the statistical average transport parameters from all of the working devices.

Molecule	Log (J at 1 V (A/cm²))	R(kΩ)	ϕ_B (eV)	α	β (Å^{-1})
Octane-S	4.87 ± 0.23	1.03 ± 0.44	1.08 ± 0.26	0.77 ± 0.08	0.81 ± 0.05
Octane-Se	4.65 ± 0.35	1.87 ± 1.45	1.15 ± 0.22	0.76 ± 0.12	0.82 ± 0.08

Note: These parameters were obtained by taking statistical averages from individual fitting parameters of all of the working devices (see text).

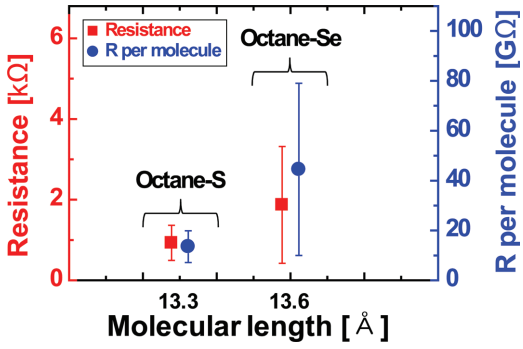

Fig. 4. Resistances of octane-S and octane-Se working molecular devices obtained from the low bias regimes with the estimated values of resistance per molecule.

octane-Se devices was wider, which is consistent with the large β value distribution due to irregular binding sites of octane-Se on Au surface. In Figure 4, we also added the values of the resistance per molecule in the right vertical axis. In this estimation, we assumed the identical unit cell area for single octane-S and octane-Se molecule on Au surface. However, this assumption may not be always true due to aforementioned irregularity of octane-Se binding sites. Given with this harsh assumption, we found the resistance per molecule is lower than that of 13.5 GΩ for octane-S and 44.5 GΩ for octane-Se because of low packing densities derived from irregularities in molecular monolayers. From these results, we can find that there is a difference electronic property between octane-S and octane-Se devices, originated from different molecular contacts, although the difference is not so significant.

4. CONCLUSION

We investigated the charge transport properties through alkyl-chain molecules having different molecular end-groups of S and Se using microscale via-hole molecular devices. From statistical analysis of a significantly large number of octane-Se devices (2240 devices), we could obtain the device yield (∼1.7% yield) and the detail electrical parameters of current, resistance, and decay coefficient. Particularly, we found that the conductance was slightly smaller and decay coefficient was slightly larger for octane-Se devices than those for octane-S devices. The standard deviations of the transport properties of octane-Se devices were found to be broader than those of octane-S devices because of irregularity of octane-Se binding sites on the Au surface.

Acknowledgment: This work was supported by National Research Laboratory (NRL) Program of the Korea Science and Engineering Foundation (KOSEF) and the Program for Integrated Molecular System at GIST.

References and Notes

1. M. A. Reed and T. Lee (eds.), Molecular Nanoelectronics, American Scientific, Stevenson Ranch **(2003)**.
2. A. Nitzan and M. A. Ratner, *Science* 300, 1384 **(2003)**.
3. J. Park, A. N. Pasupathy, J. I. Goldsmth, C. Chang, Y. Yaish, J. R. Petta, M. Rinkoski, J. P. Sethna, H. D. Abruña, P. L. McEuen, and D. C. Ralph, *Nature (London)* 417, 722 **(2002)**.
4. J. Chen, M. A. Reed, A. M. Rawlett, and J. M. Tour, *Science* 286, 1550 **(1999)**.
5. C. P. Collier, E. W. Wong, M. Belohradský, F. M. Raymo, J. F. Stoddart, P. J. Kuekes, R. S. Williams, and J. R. Heath, *Science* 285, 391 **(1999)**.
6. Y. Chen, G. Y. Jung, D. A. A. Ohlberg, X. Li, D. R. Stewart, J. O. Jeppesen, K. A. Nielsen, J. F. Stoddart, and R. S. Williams, *Nanotechnology* 14, 462 **(2003)**.
7. J. E. Green, J. W. Choi, A. Boukai, Y. Bunimovich, E. Johnston Halperin, E. Delonno, Y. Luo, B. A. Sheriff, K. Xu, Y. S. Shin, H.-R. Tseng, J. F. Stoddart, and J. R. Heath, *Nature (London)* 445, 414 **(2007)**.
8. S. Datta, W. Tian, S. Hong, R. Reifenberger, J. I. Henderson, and C. P. Kubiak, *Phys. Rev. Lett.* 79, 2530 **(1997)**.
9. J. G. Kushmerick, D. B. Holt, J. C. Yang, J. Naciri, M. H. Moore, and R. Shashidhar, *Phys. Rev. Lett.* 89, 086802 **(2002)**.
10. J. Taylor, M. Brandbyge, and K. Stokbro, *Phys. Rev. Lett.* 89, 138301 **(2002)**.
11. V. B. Engelkes, J. M. Beebe, and C. D. Frisbie, *J. Am. Chem. Soc.* 126, 14287 **(2004)**.
12. J. G. Kushmerick, *Mater. Today* 8, 26 **(2005)**.
13. A. Salomon, D. Cahen, S. Lindsay, J. Tomfohr, V. B. Engelkes, and C. D. Frisbie, *Adv. Mater. (Weinheim, Ger.)* 15, 1881 **(2003)**.
14. A. Salomon, T. Böcking, J. J. Gooding, and D. Cahen, *Nano Lett.* 6, 2873 **(2006)**.
15. T.-W. Kim, G. Wang, H. Lee, and T. Lee, *Nanotechnology* 18, 315204 **(2007)**.
16. M. T. González, S. Wu, R. Huber, S. J. Molen, C. Schönenberger, and M. Calame, *Nano Lett.* 6, 2238 **(2006)**.
17. S.-Y. Jang, P. Reddy, A. Majumdar, and R. A. Segalman, *Nano Lett.* 6, 2362 **(2006)**.
18. T.-W. Kim, G. Wang, H. Song, N.-J. Choi, H. Lee, and T. Lee, *J. Nanosci. Nanotechnol.* 6, 3487 **(2006)**.
19. J. M. Seminario, A. G. Zacarias, and J. M. Tour, *J. Am. Chem. Soc.* 121, 411 **(1999)**.
20. W. Wang, T. Lee, and M. A. Reed, *Phys. Rev. B* 68, 035416 **(2003)**.
21. J. G. Simmons, *J. Appl. Phys.* 34, 1793 **(1963)**.
22. D. J. Wold and C. D. Frisbie, *J. Am. Chem. Soc.* 123, 5549 **(2001)**.
23. X. D. Cui, X. Zarate, J. Tomfohr, O. F. Sankey, A. Primak, A. L. Moore, T. A. Moore, D. Gust, G. Harris, and S. M. Lindsay, *Nanotechnology* 13, 5 **(2002)**.
24. D. J. Wold, R. Haag, M. A. Rampi, and C. D. Frisbie, *J. Phys. Chem. B* 106, 2813 **(2002)**.
25. H. Haick, J. Ghabboun, and D. Cahen, *Appl. Phys. Lett.* 86, 042113 **(2005)**.
26. N. Majumdar, N. Gergel, D. Routenberg, J. C. Bean, L. R. Harriott, B. Li, L. Pu, Y. Yao, and J. M. Tour, *J. Vac. Sci. Technol. B* 23, 1417 **(2005)**.
27. J. D. Monnell, J. J. Stapleton, J. J. Jackiw, T. Dunbar, W. A. Reinerth, S. M. Dirk, J. M. Tour, D. L. Allara, and P. S. Weiss, *J. Phys. Chem.* B 108, 9834 **(2004)**.
28. T. Nakamura, T. Miyamae, D. Yoshimura, N. Kobayashi, H. Nozoye, and M. Matsumoto, *Langmuir* 21, 5026 **(2005)**.
29. S. W. Han, S. J. Lee, and K. Kim, *Langmuir* 17, 6981 **(2001)**.
30. A. Ulman, Thin Films: Self-Assembled Monolayers of Thiols, Academic Press, Sandiego, CA **(1998)**.

Received: 30 May 2008. Accepted: 19 January 2009.